

## Article

# Predicting the Distributions of *Morus notabilis* C. K. Schneid under Climate Change in China

Hui Gao <sup>1,†</sup>, Qianqian Qian <sup>2,†</sup>, Xinqi Deng <sup>2</sup>, Yaqin Peng <sup>2</sup> and Danping Xu <sup>1,2,\*</sup>

<sup>1</sup> College of Environmental Science and Engineering, China West Normal University, Nanchong 637002, China; hubeihuige@cwnu.edu.cn

<sup>2</sup> College of Life Science, China West Normal University, Nanchong 637002, China; qianqqq520@gmail.com (Q.Q.); senkykalivan@gmail.com (X.D.); pengyaqin36@gmail.com (Y.P.)

\* Correspondence: xudanping@cwnu.edu.cn; Tel.: +86-15008315762

† These authors contributed equally to this work.

**Abstract:** As one of the common mulberry tree species, *Morus notabilis* C. K. Schneid plays a significant role in various industries such as silkworm rearing, papermaking, and medicine due to its valuable mulberry leaves, fruits, and wood. This study utilizes the maximum entropy (MaxEnt) model to predict the potential distribution of *M. notabilis* in China under future environmental changes. By integrating the relative percentage contribution score of environmental factors with jackknife test analysis, important variables influencing the distribution of *M. notabilis* were identified along with their optimal values. The results indicate that Annual Precipitation (bio12), Precipitation of Driest Month (bio14), Min Temperature of Coldest Month (bio6), Temperature Annual Range (bio5–bio6) (bio7), Precipitation of Warmest Quarter (bio18), and Precipitation of Coldest Quarter (bio19) are the primary environmental variables affecting its potential distribution. Currently, *M. notabilis* exhibits high suitability over an area spanning 11,568 km<sup>2</sup>, while medium suitability covers 34,244 km<sup>2</sup>. Both current and future suitable areas for *M. notabilis* are predominantly concentrated in Sichuan, Yunnan, and Guizhou provinces, as well as Chongqing city in southwest China. Under the SSP5-8.5 scenario representing high greenhouse gas concentrations by 2050s and 2090s, there is an increase in high suitability area by 2952 km<sup>2</sup> and 3440 km<sup>2</sup>, with growth rates reaching 25.52% and 29.74%, respectively. Notably, these two scenarios exhibit substantial expansion in suitable habitats for this species compared to others analyzed within this study period.

**Keywords:** MaxEnt; environmental variables; suitable habitats; potential distribution area; habitat suitability simulation



**Citation:** Gao, H.; Qian, Q.; Deng, X.; Peng, Y.; Xu, D. Predicting the Distributions of *Morus notabilis* C. K. Schneid under Climate Change in China. *Forests* **2024**, *15*, 352. <https://doi.org/10.3390/f15020352>

Academic Editors: Nadezhda Tchebakova and Sergey V. Verkhovets

Received: 8 January 2024

Revised: 7 February 2024

Accepted: 8 February 2024

Published: 11 February 2024



**Copyright:** © 2024 by the authors. Licensee MDPI, Basel, Switzerland. This article is an open access article distributed under the terms and conditions of the Creative Commons Attribution (CC BY) license (<https://creativecommons.org/licenses/by/4.0/>).

## 1. Introduction

*Morus notabilis* C.K. Schneid (Moraceae) is a species of mulberry. Mulberry leaves are a crucial economic feed crop for silkworms [1]. The delectable taste of mulberry fruits is highly regarded [2]. Mulberry paper, derived from the bark of the mulberry tree, was initially produced and utilized during the Han Dynasty [3]. With medicinal value in all its parts, mulberry trees hold significant importance as one of China's key crops. Originating from China's vast land, mulberry cultivation and sericulture boast a long-standing history [4]. These popular trees thrive in diverse climates and complex terrain within an ecological environment. Over time, the germplasm resources of mulberry trees have been meticulously selected through artificial means [5,6], also known as round leaf or hairy vein mulberry, which represents one common variety with deciduous characteristics [7,8]. *M. notabilis* predominantly thrives in mountain valleys, forests, and canyons where it coexists with broad-leaved forests; however, its distribution area necessitates high humidity levels found specifically in high-altitude regions [9].

Currently, research on *M. notabilis* primarily focuses on its biological characteristics and genetic improvement, with no available research reports predicting its potential distribution [10,11]. The spatial distribution area of a species is a crucial ecological and evolutionary characteristic. In addition to traditional field investigations, studying species distribution has opened up new avenues for research [12]. By establishing an ecological niche model based on the theory of ecological niche, we can better understand and apply this species. The niche model predicts the future distribution of a species by examining the relationship between its existence and environmental variables, thereby determining its potential distribution area in the future [13,14]. Among various niche models, the MaxEnt model stands out due to its advantages, such as its small sample size requirements and accurate predictions [15]. The short run time, ease of operation, and high accuracy were also important reasons for choosing this model [16]. The MaxEnt model has been used for different species in different countries, for example, Thakur et al. [17] predicted suitable distribution areas for *Elwendia persica* (Boiss.) in the Indian Himalayan region, and Ji et al. [18] predicted suitable distribution areas for *Daktulosphaira vitifoliae* (Fitch) globally. In this study, we employ the MaxEnt model along with ArcGIS technology to predict both current and future potential suitability distribution areas for *M. notabilis* under different climate conditions [19,20]. This analysis aims to elucidate how environmental changes impact the distribution patterns of *M. notabilis* while providing a solid foundation for further research on this species.

## 2. Materials and Methods

### 2.1. Species Data Sources and Processing

*M. notabilis*, which is native to China, mainly distributes in the Sichuan, Yunnan, and Guizhou provinces of China. In order to better understand the distribution of *M. notabilis*, the information on *M. notabilis* was downloaded from the Global Biodiversity Information Service (GBIF, <https://www.gbif.org/>, accessed on 12 January 2022) in this study [21]. The retrieved distribution data were preliminary compared with the existing literature on this species, and the latitude and longitude information of each distribution point was further determined on Google Earth (<http://www.earthol.com/>, accessed on 12 January 2022). The obtained geographic distribution data are the basic information for studying the ecology of *M. notabilis* species. Strong spatial correlation between points would result in overfitting. Buffer analysis was used to set the spatial resolution of environmental data at 2.5 arc-min (about 4.5 km), and the buffer radius of 1.5 km was screened in ArcGIS 10.8 software (Environmental Systems Research Institute, for USA, state of California) [22]. Finally, a total of 101 effective distribution points of mulberry were obtained (Figure 1). Referring to the MaxEnt 3.4.4 operation manual ([https://biodiversityinformatics.amnh.org/open\\_source/maxent/](https://biodiversityinformatics.amnh.org/open_source/maxent/), accessed on 12 January 2022, RRID: SCR\_021830), the longitude and latitude coordinates were input into Excel and saved as \*.CSV format [23].

### 2.2. Environmental Factors

The distribution of biological populations and the formation of ecological niches are influenced by multiple factors, with environmental factors being particularly significant. To comprehensively analyze the impact of the environment on the distribution of *M. notabilis* in China, this study selected natural environmental factors from various aspects, including bioclimate, topography, soil, and chemistry [24]. These factors were observed for their influence on the distribution patterns of *M. notabilis* in China. A total of 19 bioclimatic variables (bio1–bio19) reflecting precipitation and temperature characteristics were chosen from the world's climate database (<http://www.worldclim.org/>, accessed on 12 January 2022). In order to avoid autocorrelation between variables, a jackknife test was conducted using MaxEnt 3.4.4 software (American Museum of Natural History, for USA, state of New York) to identify dominant variables with higher contribution rates to the model (Table 1) [25,26]. Following this test, two environmental variables (bio2 and bio17) that made no contribution to the model were removed. Spearman correlation coefficient analysis

was then employed to examine correlations among the remaining 17 bioclimatic variables in order to enhance model prediction accuracy. Variables with correlation coefficients  $|r| < 0.8$  were selected, while those with significant correlations  $|r| \geq 0.8$  were identified as important environmental factors contributing to the model outcome. Based on results from both tests mentioned above, nine out of the initial 19 bioclimatic variables remained along with other terrain-related, soil-related, and chemistry-related environmental factors (Table 2), which together constituted inputs for modeling and analysis using MaxEnt. Soil variables are obtained from the Food and Agriculture Organization (FAO, <https://www.fao.org/soils-portal/en/>, accessed on 25 January 2022). Terrain variables are available from the National Oceanic and Atmospheric Administration (NOAA, <https://www.noaa.gov/>, accessed on 25 January 2022). Chemical variables are available from the World Ozone and Ultraviolet Radiation Data Centre (WOUDC, <https://woudc.org/home.php>, accessed on 25 January 2022). Human variables can be downloaded from the Center for International Earth Science Information Network (CIESIN, <http://www.ciesin.org/>, accessed on 25 January 2022).

**Table 1.** Percentage contribution and ranking importance of screened climate variables. Percent contribution and permutation importance are used as measures to determine the importance of input variables in the final model.

Bio-Climatic Variables	Abbreviation	Percent Contribution/%	Permutation Importance/%
Annual Precipitation	Bio12	39.8	0.3
Min Temperature of Coldest Month	Bio6	18.1	0
Temperature Annual Range (bio5–bio6)	Bio7	13	3.3
Precipitation of Coldest Quarter	Bio19	10.5	11.4
Precipitation of Warmest Quarter	Bio18	8.1	1.8
Max Temperature of Warmest Month	Bio5	3.4	6
Precipitation Seasonality (Coefficient of Variation)	Bio15	2.7	1.5
Mean Temperature of Driest Quarter	Bio9	1.1	12.5
Precipitation of Driest Month	Bio14	1.1	2.3
Isothermality (bio 2/bio 7) (*100)	Bio3	0.8	1.7
Mean Temperature of Warmest Quarter	Bio10	0.5	4.1
Temperature Seasonality (SD *100)	Bio4	0.4	48.5
Precipitation of Wettest Quarter	Bio16	0.2	0
Precipitation of Wettest Month	Bio13	0.1	1.4
Mean Temperature of Wettest Quarter	Bio8	0.1	3.1
Annual Mean Temperature	Bio1	0.1	1.3
Mean Temperature of Coldest Quarter	Bio11	0.1	1
Mean Diurnal Range (Mean of monthly [max temp–min temp])	Bio2	0	0
Precipitation of Driest Quarter	Bio17	0	0

The BCC-CSM1-1 coupling model (affiliated with the National Climate Center) selected for this experiment is considered the optimal choice among global climate models for regional climate simulation in China. Future climate data for the 2050s (2041s–2060s) and 2090s (2081s–2100s) were obtained from the Climate Change, Agriculture and Food Security website (CCAFS, <https://ccafs.cgiar.org/>, accessed on 25 January 2022). Based on different shared socio-economic pathways (SSPs), as outlined in the IPCC's fifth report, four typical greenhouse gas concentration scenarios exist. In this study, three scenarios, namely SSP1-2.6, SSP2-4.5, and SSP5-8.5, were selected to model the future suitable distribution areas of *M. notabilis*. SSP1-2.6 is a significant cut in global CO<sub>2</sub> emissions, reaching net zero after 2050; SSP2-4.5 is CO<sub>2</sub> emissions hovering at current levels until they begin to decline in the middle of the century but do not reach net zero by 2100; and SSP5-8.5 is a level of CO<sub>2</sub> emissions that roughly doubles by 2050 (ICPP, <http://www.icpp.ch/report/ar6/wg1>, accessed on 25 January 2022).

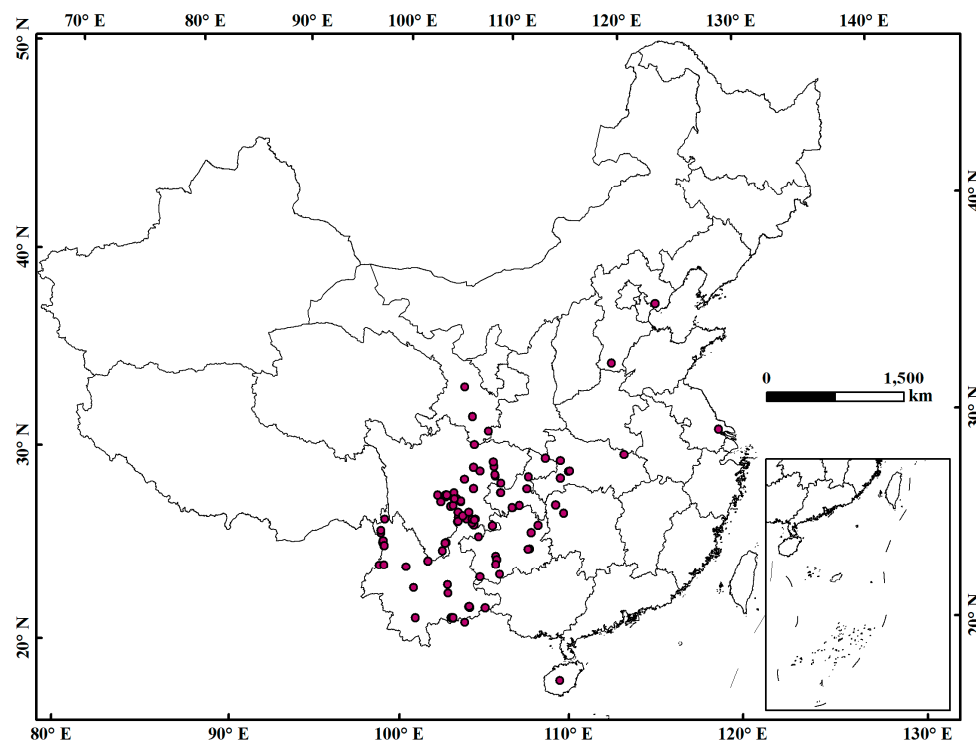


**Figure 1.** Geographical distribution points of *Morus notabilis* C.K. Schneid.

**Table 2.** Environmental variables used to predict the distribution of *Morus notabilis* C. K. Schneid.

Variable Classification	Environmental Variables	Unit	Abbreviation
Bio-climatic variables	Annual Precipitation	mm	Bio12
	Min Temperature of Coldest Month	°C	Bio6
	Temperature Annual Range (bio5–bio6)	°C	Bio7
	Precipitation of Coldest Quarter	mm	Bio19
	Precipitation of Warmest Quarter	mm	Bio18
	Max Temperature of Warmest Month	°C	Bio5
	Precipitation Seasonality (Coefficient of Variation)	mm	Bio15
	Precipitation of Driest Month	mm	Bio14
	Isothermality (bio 2/bio 7) (×100)	×100	Bio3
Soil variables	Soil reference depth	/	Ref-depth
	Soil acidity and alkalinity	/	pH
	Upper soil sediment content	%wt.	T-sand
	Organic carbon content	%wt.	TOC
	Soil evaluation indicators	/	USDA
Terrain variables	The orientation of the terrain slope	Degree	Aspect
	The degree of steepness and gentleness of surface units	°	Slope
	Altitude	m	Alt
Chemical variables	Ultraviolet-B radiation	nm	UV-B
Human variables	Human footprint	/	Hf

### 2.3. MaxEnt Modeling

Utilizing MaxEnt model software version 3.4.4., a total of 101 effective distribution points along with 19 environmental factors were selected and imported to simulate potential distributions of *M. notabilis* both presently and in future scenarios. Training data sets comprised randomly selected species occurrence data amounting to 75%, while remaining species data constituted test data sets comprising 25%. Additionally, ten repetitions of training were conducted to mitigate any random aberrations. The receiver operating characteristic (ROC) curve was obtained by the jackknife test. The area under the ROC curve surrounded by the coordinate axis, that is, the area under the curve (AUC) value, was

used as the judgment basis to evaluate the model simulation results. It generally ranges from 0.5 to 1. The AUC value is taken as the average of 10 tests. The closer the value is to 1, the better the model's prediction is, and between 0.70 and 0.80, it indicates an average prediction. A range of 0.81 to 0.90 indicates that the prediction results are accurate. A value between 0.91 and 1.00 indicates that the prediction is very accurate.

#### 2.4. Classification of Suitable Grades

Combining with the results of the MaxEnt model, the suitability distribution of Mulberry in our country was analyzed by ArcGIS software. According to the probabilistic classification According to the methodology developed by the IPCC in 2007, four separate colors are used to indicate habitat suitability status: inappropriate area (white,  $p < 0.05$ ), low suitability area (yellow,  $0.05 < p < 0.33$ ), medium suitability area (green,  $0.33 < p < 0.66$ ), and high suitability area (blue,  $0.66 < p < 1$ ).

### 3. Results

#### 3.1. Model Optimization Results and Accuracy Evaluation

The ROC curve is a graphical tool that depicts the performance of a model, and the AUC value represents the area under the ROC curve. In this study, the MaxEnt model was employed twice to generate corresponding ROC curves. The validation results of 19 bioclimatic variables (bio1–bio19), introduced for the first time, demonstrated that the AUC value for the training set was 0.945, while it was 0.943 for the test set (Figure 2). Furthermore, averaging across both predictions based on dominant climate variables and other environmental factors such as terrain, soil, and chemistry yielded an average AUC value of 0.938 (Figure 3). Both AUC values fell within the range of 0.9~1.0, indicating highly accurate predictions by the MaxEnt model.

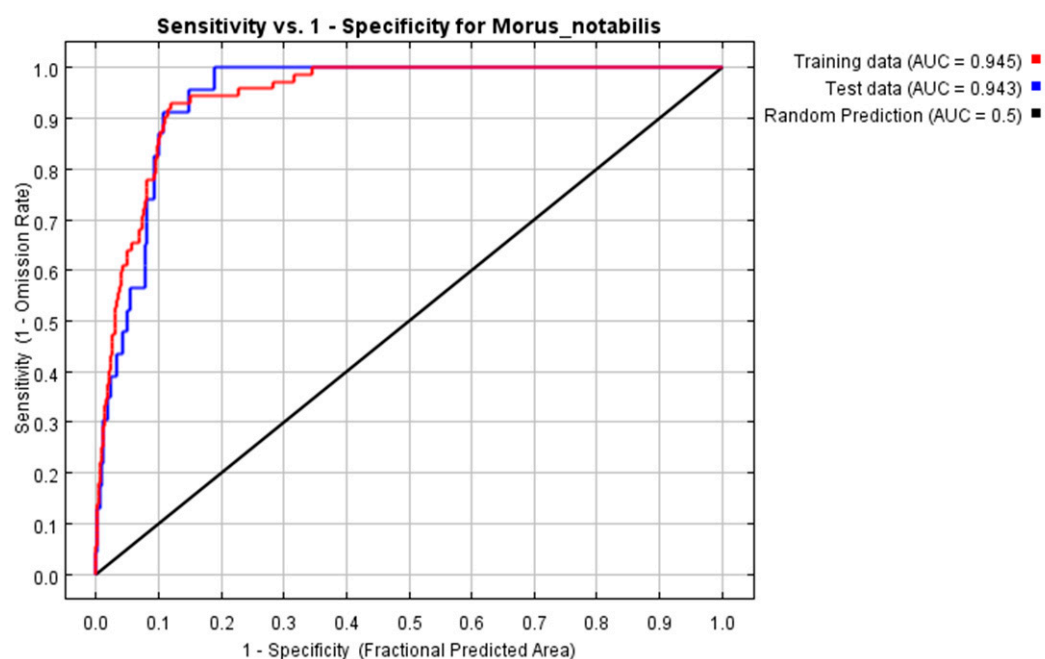


**Figure 2.** ROC curve verification of 19 bioclimatic variables.

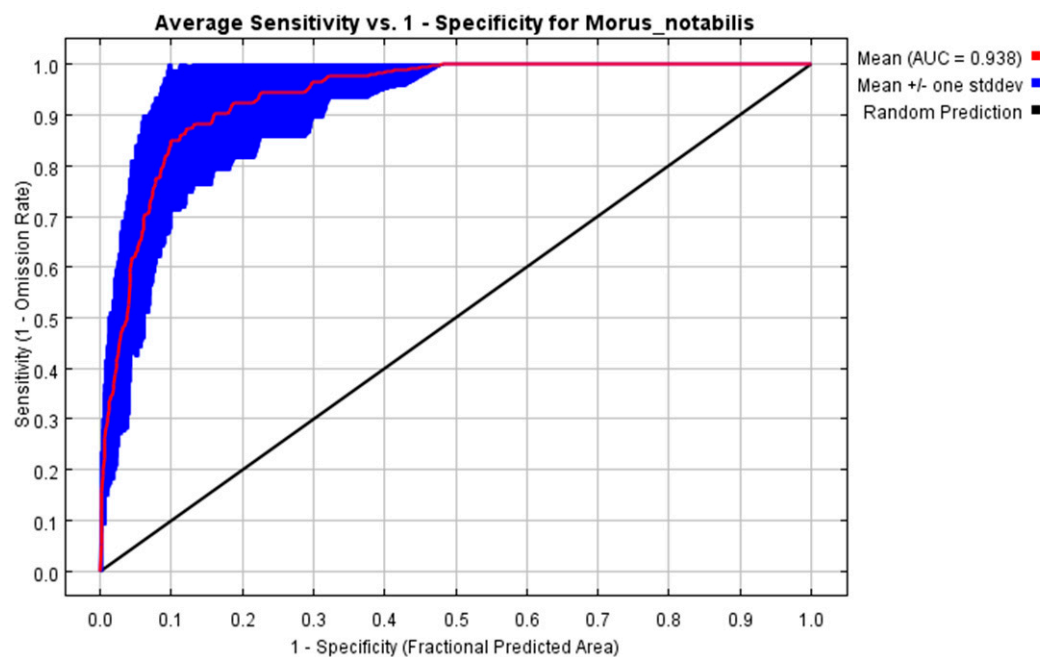


**Figure 3.** ROC curve of potential distribution prediction for *Morus notabilis* C. K. Schneid.

### 3.2. Model Performance and Key Environment Variables

In total, this study selected 19 environmental variables, comprising nine significant bioclimatic variables and ten related to terrain, soil, chemistry, and other environmental factors. The relative contribution values of these variables were calculated using the Maxent model (refer to Table 3). Annual Precipitation (bio12) exhibited the highest contribution rate at 42.6%. Other environmental variables with relative contribution rates exceeding 1% included Altitude, Min Temperature of Coldest Month (bio6), Human footprint (hf), Temperature Annual Range (bio5–bio6) (bio7), Precipitation of Coldest Quarter (bio19), ultraviolet-B radiation (UV-B), Precipitation of Driest Month (bio14), Precipitation of Warmest Quarter (bio18), and Soil reference depth (Ref-depth). Cumulatively accounting for these ten variables, which amounted to a contribution rate of approximately bioclimatic environmental factors with relatively high correlation, has been performed using Spearman correlation analysis, and variables with relatively low impact have been omitted from variables with high correlation. Moreover, 19 environmental variables continue to be put into the MaxEnt model for modeling.

**Table 3.** Contribution percentage and ranking importance of environmental variables affecting the distribution of *Morus notabilis* C. K. Schneid.

Variable Classification	Abbreviation	Percent Contribution/%	Permutation Importance/%
Annual Precipitation	Bio12	42.6	0.4
Altitude	alt	11	8.8
Min Temperature of Coldest Month	Bio6	9.2	26.3
Human footprint	hf	8.5	6.1
Temperature Annual Range (bio5–bio6)	Bio7	7.5	19.4
Precipitation of Coldest Quarter	Bio19	5.7	15.2
Ultraviolet-B radiation	UV-B	4.5	5.8
Precipitation of Driest Month	Bio14	3.8	7.2
Precipitation of Warmest Quarter	Bio18	3	3.2
Soil reference depth	Ref-depth	1	0.7
Soil acidity and alkalinity	pH	0.8	1.8
Precipitation Seasonality (Coefficient of Variation)	Bio15	0.5	0.2

Table 3. Cont.

Variable Classification	Abbreviation	Percent Contribution/%	Permutation Importance/%
The orientation of the terrain slope	Aspect	0.4	1.1
Soil evaluation indicators	USDA	0.4	0.1
Upper soil sediment content	T-sand	0.3	2.1
Max Temperature of Warmest Month	Bio5	0.3	1
Isothermality (bio 2/bio 7) ( $\times 100$ )	Bio3	0.1	0.6
Organic carbon content	TOC	0.1	0.1
The degree of steepness and gentleness of surface units	Slope	0	0

### 3.3. Predicting the Current Distribution of *Morus notabilis* C. K. Schneid in China

The 101 effective distribution points of *M. notabilis* were imported and analyzed using the Maxent model combined with environmental variables. Results showed that under current climate conditions, the distribution of *M. notabilis* in China exhibits high, medium, low, and poor suitability (Figure 4). Highly suitable areas are concentrated in the Sichuan, Yunnan, Guizhou, Chongqing, and Hubei provinces, with a total area of  $20.08 \times 10^4 \text{ km}^2$  or 39.33% of China's land area (Table 4). Sichuan is the main high-suitability region for *M. notabilis*, accounting for 45.18% of all high-suitability areas in China, while Yunnan-Guizhou Plateau has a total area of  $10.19 \times 10^4 \text{ km}^2$  or about half (50.73%) of all high-suitability regions in China; these two regions account for almost all (95.91%) highly suitable areas nationwide, indicating that they are mainly located in southwest China along the upper reaches of the Yangtze River, characterized by subtropical monsoon climate conditions. It is estimated that the total area of moderately suitable areas is about  $59.45 \times 10^4 \text{ km}^2$ , accounting for about 6.21% of China's land area, and mainly distributed in the southwestern region, Hubei, Hunan, and other areas close to the border of the southwestern region, with a small amount distributed in the southern region of China, such as Guangxi and Taiwan. The southwestern region includes Yunnan, Sichuan, Guizhou, Chongqing, and Tibet, accounting for 88.17% of the total area of moderately suitable land in China. In contrast to the concentrated distribution of highly and moderately suitable areas, low-suitability areas are widely dispersed across regions such as Guangxi, Henan, and Shaanxi, as well as the Southwest, South Central East, and North China. Among all provinces in China surveyed for this study, Chongqing exhibits the highest proportion of highly suitable land (29.13%), followed by Sichuan with 19.93%. Additionally, Chongqing has a remarkable percentage (100%) of its total provincial area classified as suitable land, surpassing other provinces like Guizhou, Yunnan, and Hainan, where over 90% is deemed suitable.

**Table 4.** Predicted suitability for *Morus notabilis* C. K. Schneid in China under current climatic conditions.

Province	High Suitable Area ( $10^4 \text{ km}^2$ )	Medium Suitable Area ( $10^4 \text{ km}^2$ )	Low Suitable Area ( $10^4 \text{ km}^2$ )	Percentage of High Suitable Areas in Province (%)	Percentage of Suitable Areas in Province (%)
Sichuan	9.07	10.40	7.36	19.93	58.94
Yunnan	3.55	22.63	7.73	10.34	98.88
Guizhou	2.79	9.32	3.80	17.47	99.66
Chongqing	2.25	4.92	0.56	29.13	100.00
Hubei	1.60	3.24	7.75	9.12	71.74
Xinjiang	0.48	1.90	6.64	0.42	7.90
Guangxi	0.13	2.43	10.08	0.62	60.42
Shanxi	0.10	1.61	8.93	0.49	52.22
Taiwan	0.04	0.45	1.53	1.27	64.02
Hunan	0.02	0.66	5.11	0.13	29.91

Table 4. Cont.

Province	High Suitable Area (10 <sup>4</sup> km <sup>2</sup> )	Medium Suitable Area (10 <sup>4</sup> km <sup>2</sup> )	Low Suitable Area (10 <sup>4</sup> km <sup>2</sup> )	Percentage of High Suitable Areas in Province (%)	Percentage of Suitable Areas in Province (%)
Gansu	0.02	0.36	3.66	0.05	9.74
Shandong	0.01	0.34	6.43	0.07	44.24
Hainan	0.01	0.11	2.40	0.19	92.89
Jiangsu	0.00	0.17	5.38	0.04	57.60
Guangdong	0.00	0.13	7.89	0.01	52.48
Henan	0.00	0.29	9.97	0.01	63.63
Tianjin	0.00	0.06	0.47	0.14	43.73
Anhui	0.00	0.13	5.25	0.00	40.28
Beijing	0.00	0.07	0.67	0.00	42.64
Fujian	0.00	0.02	4.60	0.00	42.75
Hebei	0.00	0.07	2.87	0.00	14.97
Heilongjiang	0.00	0.00	0.00	0.00	0.01
Jilin	0.00	0.00	0.05	0.00	0.24
Jiangxi	0.00	0.00	0.27	0.00	1.80
Liaoning	0.00	0.05	1.65	0.00	10.90
Inner Mongolia	0.00	0.00	0.02	0.00	0.02
Ningxia	0.00	0.00	0.06	0.00	1.09
Qinghai	0.00	0.00	0.13	0.00	0.18
Shaanxi	0.00	0.08	3.77	0.00	24.12
Shanghai	0.00	0.00	0.26	0.00	44.48
Xizang	0.00	0.00	0.01	0.00	0.00
Zhejiang	0.00	0.00	1.01	0.00	10.88
China	20.08	59.45	116.32	39.33	20.85

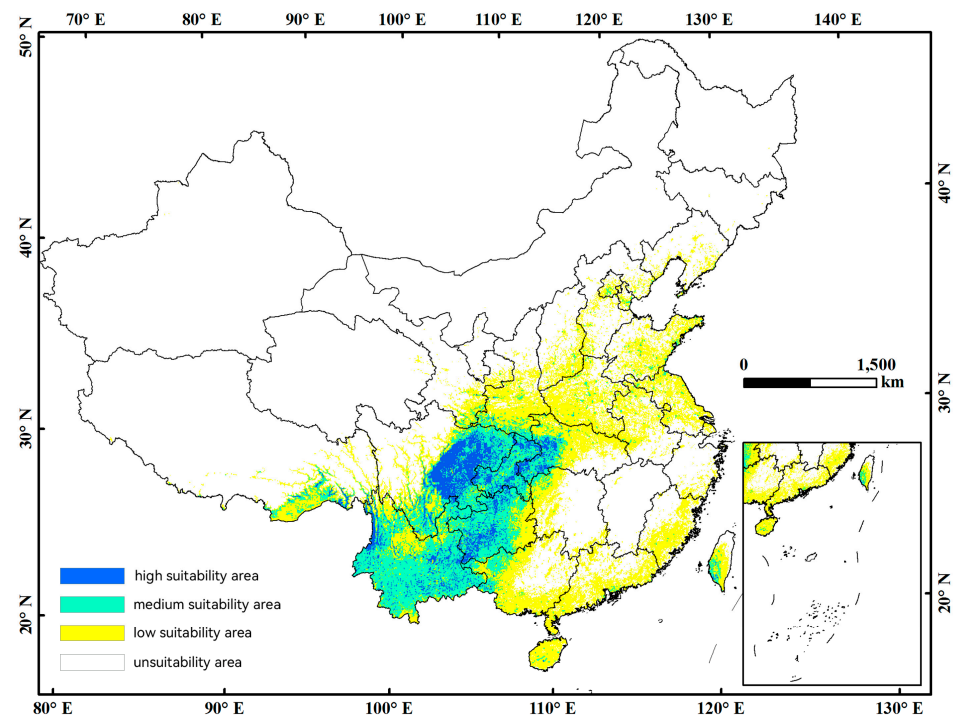


**Figure 4.** Current suitable climatic distribution of *Morus notabilis* C. K. Schneid in China. The probability of *M. notabilis* is shown by the color scale in the area. Blue indicates a highly suitable area with a probability of higher than 0.66, light green indicates a moderately suitable area with a probability of 0.33–0.66, yellow indicates a poorly suitable area with a probability ranging from 0.05–0.33, and white represents unsuitable areas.

### 3.4. Potential Distribution of *Morus notabilis* C. K. Schneid in the Future Period

In this study, the representative years for future prediction of *M. notabilis* were selected as the 2050s and 2090s. Figure 5 shows the distribution of *M. notabilis* at different times in each of the three SSP scenarios. Comparing with the current suitability distribution of *M. notabilis*, both high- and low-suitability areas are projected to expand in the 2050s and 2090s. Among all climate conditions, the high suitability area experienced maximum expansion under the high SSP5-8.5 scenario. By the 2050s, a significant spread of high-suitability areas is anticipated towards Guizhou and Yunnan provinces in southwest China, while primarily concentrated in Sichuan and Yunnan provinces, supplemented by Guizhou, Chongqing, and Hubei provinces; other regions show relatively less distribution at this time point. By the year 2090s, a direct concentration of high-suitable areas is expected in Guizhou province, mainly distributed across Sichuan and Guizhou, with supplementary presence in Yunnan and Chongqing provinces. The current  $2.79 \times 10^4$  km<sup>2</sup> of Guizhou will increase to  $7.63 \times 10^4$  km<sup>2</sup> in the 2090s, and the proportion of high-suitable area in the total area of the province will increase from 17.47% to 47.82%, with an increase rate of 173.73%. Based on the data analysis of the future suitability changes of *M. notabilis*, as shown in Table 5, in the 2050s and 2090s, the areas of high suitability and low suitability will increase to varying degrees under the three SSP climate changes, while the areas of medium suitability will decrease to varying degrees. As a whole, the total area of all suitable areas, including high, medium, and low, will increase under all scenarios predicted in this study, among which the SSP2-4.5 climate change in the 2050s will increase the area the most, with a total increase of  $15.65 \times 10^4$  km<sup>2</sup>.

**Table 5.** Predicted suitable areas for *Morus notabilis* C. K. Schneid under current and future climatic conditions.

Decade	Scenarios	Predicted Area (10 <sup>4</sup> km <sup>2</sup> )			Comparison with Current Distribution (%)		
		High Suitable	Medium Suitable	Low Suitable	High Suitable	Medium Suitable	Low Suitable
Current	-	20.08	59.45	116.32	-	-	-
2050s	SSP1-2.6	21.79	54.29	122.98	8.51	-8.68	5.72
	SSP2-4.5	21.33	56.83	133.35	6.21	-4.40	14.63
	SSP5-8.5	25.21	53.19	123.66	25.52	-10.53	6.30
2090s	SSP1-2.6	22.00	54.08	127.50	9.53	-9.04	9.60
	SSP2-4.5	24.97	49.94	128.63	24.34	-15.99	10.58
	SSP5-8.5	26.06	48.99	128.36	29.74	-17.60	10.35

SSP2-2.6 represents the low-concentration climate scenario. Under this scenario in the 2050s, there will be an increase of  $6.66 \times 10^4$  km<sup>2</sup> and  $1.71 \times 10^4$  km<sup>2</sup> in the high-suitable area and low-suitable area, respectively, compared to the current distribution, resulting in an increase ratio of 8.51% and 5.72%. In the scenario of the 2090s, it is predicted that both high-suitable areas and low-suitable areas will experience a respective increase of 9.53% and 9.60% compared to their current distribution, with changes similar to those observed in the 2050s. The expansion of these suitability changes under low concentration conditions was minimal and not regionally significant. Under SSP2-4.5, representing the medium concentration climate scenario, *M. notabilis* exhibits small increases in both high suitability (6.21%) and medium suitability (-4.40%) areas relative to its current suitable range; however, there is a substantial expansion (14.63%) in low-suitability areas towards Anhui, Shandong, Henan, and other regions in East China. In the 2090s, predictions show more pronounced changes than those observed for the 2050s; specifically, there is a significant increase (24.34%) in high-suitability areas by approximately  $4.89 \times 10^4$  km<sup>2</sup> mainly concentrated in Guizhou and Yunnan provinces. The high-concentration climate scenario is represented by SSP5-8.5. Under this scenario, the predicted distribution of different suitability areas for *M. notabilis* exhibits the most significant changes compared to its current distribution [27]. In the 2050s and 2090s, the high-suitability areas will increase by  $5.13 \times 10^4$  km<sup>2</sup> and  $5.97 \times 10^4$  km<sup>2</sup>, respectively, with an increase ratio of 25.52%

and 29.74%. Among the three climate conditions considered, SSP5-8.5 shows the highest decrease in medium-suitable regions, with a decrease ratio of 17.60% in the 2090s due to their conversion into high-suitable regions primarily in Yunnan and Guizhou provinces.

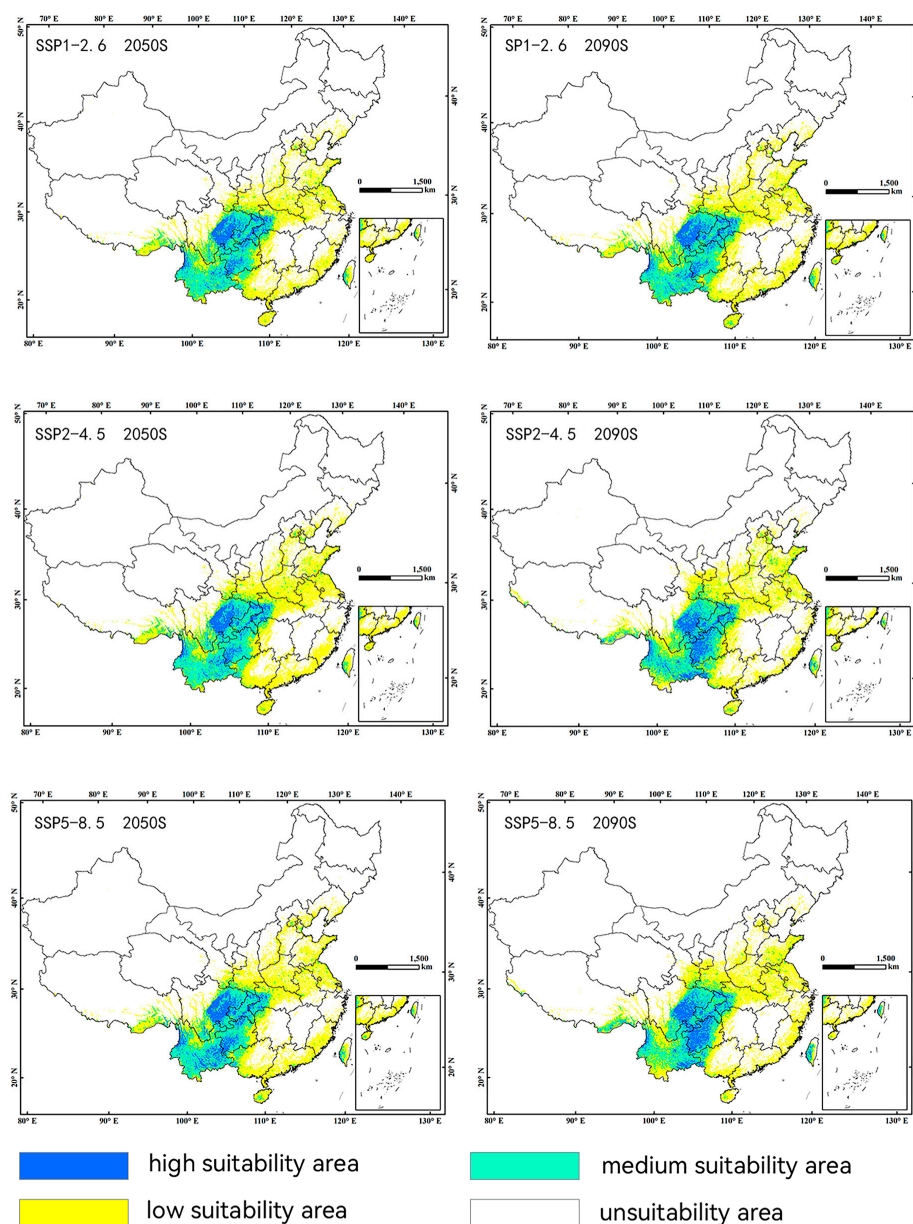


**Figure 5.** Potential distribution of *Morus notabilis* C. K. Schneid in the future period (2050s and 2090s) under the SSP1-2.6, SSP2-4.5, and SSP5-8.5 climate change scenarios. Blue indicates a highly suitable area with a probability of higher than 0.66, light green indicates a moderately suitable area with a probability of 0.33–0.66, yellow indicates a poorly suitable area with a probability ranging from 0.05 to 0.33, and white represents unsuitable areas.

### 3.5. Environmental Variable Analysis

According to preliminary screening work, a total of 19 environmental impact factors, including climate, terrain, soil, and chemistry, were selected as inputs for modeling using the MaxEnt model (Figure 6). The jackknife test revealed that all 19 selected environmental variables significantly influenced the potential distribution of *M. notabilis* to varying degrees. Analyzing the “with only variable”, “without variable”, and “with all variables” scenarios depicted in Figure 6 reveals that each individual environmental

variable contributes differently towards species' distribution potential, as indicated by blue strip lengths representing their importance when used alone. Consequently, Annual Precipitation (bio12), Precipitation of Driest Month (bio14), Min Temperature of Coldest Month (bio6), Temperature Annual Range (bio5–bio6) (bio7), Precipitation of Warmest Quarter (bio18), and Precipitation of Coldest Quarter (bio19) emerged as six key environmental variables exerting substantial influence on *M. notabilis* potential distribution.

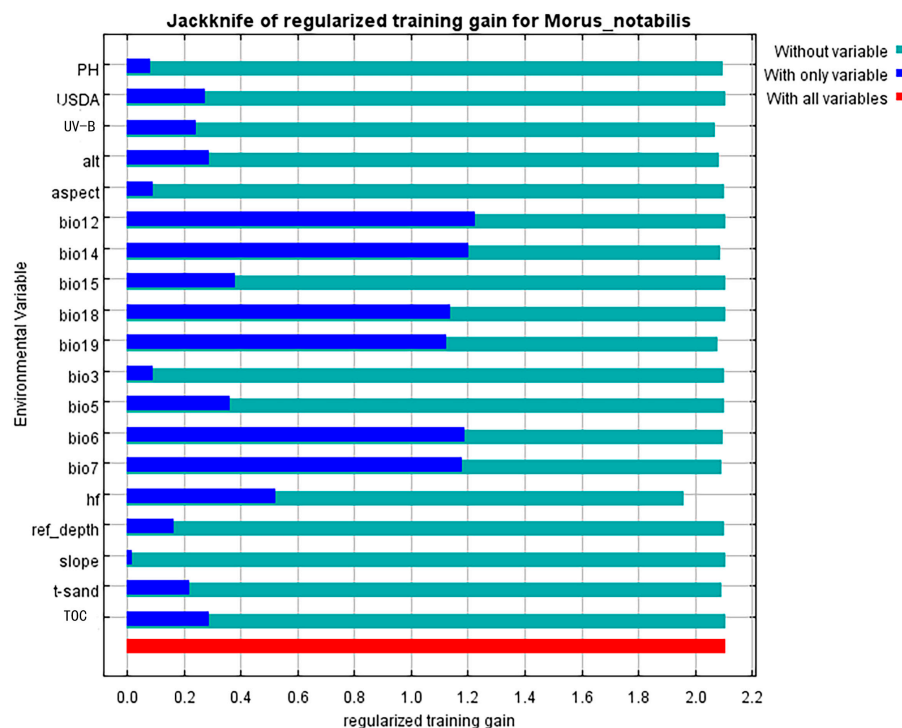


**Figure 6.** Importance of environmental variables to *Morus notabilis* by the Jackknife test.

According to the probability division method determined by the IPCC (IPCC, 2007), a threshold of 0.33 is considered the lower limit for suitability regions. Figure 7 shows the response curves of key environmental variables with respect to the probability of distribution of *M. notabilis*, indicating that the suitability of the species varies with the environment. The figure reveals an optimal value within an appropriate range for each environmental variable's influence on suitability distribution, resulting in the highest probability of suitability distribution.

Based on this distribution probability response curve, we further determine the suitable range of potential distributions for each variable related to *M. notabilis* within our research and testing scope (refer to Table 6). Analysis of the precipitation response curve during the warmest quarter reveals that *M. notabilis* cannot survive in environments with insufficient rainfall but has a relatively good tolerance for excessive water under sufficient sunlight conditions. In the coldest region, variations in precipitation response curves are similar to those observed during the driest month, with a small range between 27.53 mm and 124.09 mm; an appropriate value of 0.92 is achieved at a precipitation level of 56.68 mm. The adaptive response curves of annual precipitation, precipitation in the driest month, and precipitation in the coldest area exhibit a distinct peak, with sharp rises and falls at the zero point of the vertical axis and a narrow range of variation. This indicates that precipitation directly influences the growth of *M. notabilis*, which has strict requirements for suitable growth conditions. Insufficient or excessive water is unsuitable for its growth. Consequently, the suitability distribution of *M. notabilis* is scarcely found in Inner Mongolia due to low and uneven precipitation as well as drastic seasonal changes, as well as in Xinjiang, where a dry climate leads to scarce rainfall. The minimum temperature during the coldest month ranges from  $-6.05$  °C to  $12.05$  °C; however, it is virtually absent when

temperatures drop below  $-17\text{ }^{\circ}\text{C}$ . The optimal temperature for *M. notabilis* is  $2.58\text{ }^{\circ}\text{C}$  with a corresponding suitability value of 0.79; above this threshold ( $15.89\text{ }^{\circ}\text{C}$ ), the suitability value remains constant at 0.19, indicating unsuitability for growth conditions. The annual temperature suitable range spans from  $10.00\text{ }^{\circ}\text{C}$  to  $31.02\text{ }^{\circ}\text{C}$ , reaching its peak suitability value at  $26.50\text{ }^{\circ}\text{C}$  before rapidly declining with further increases.

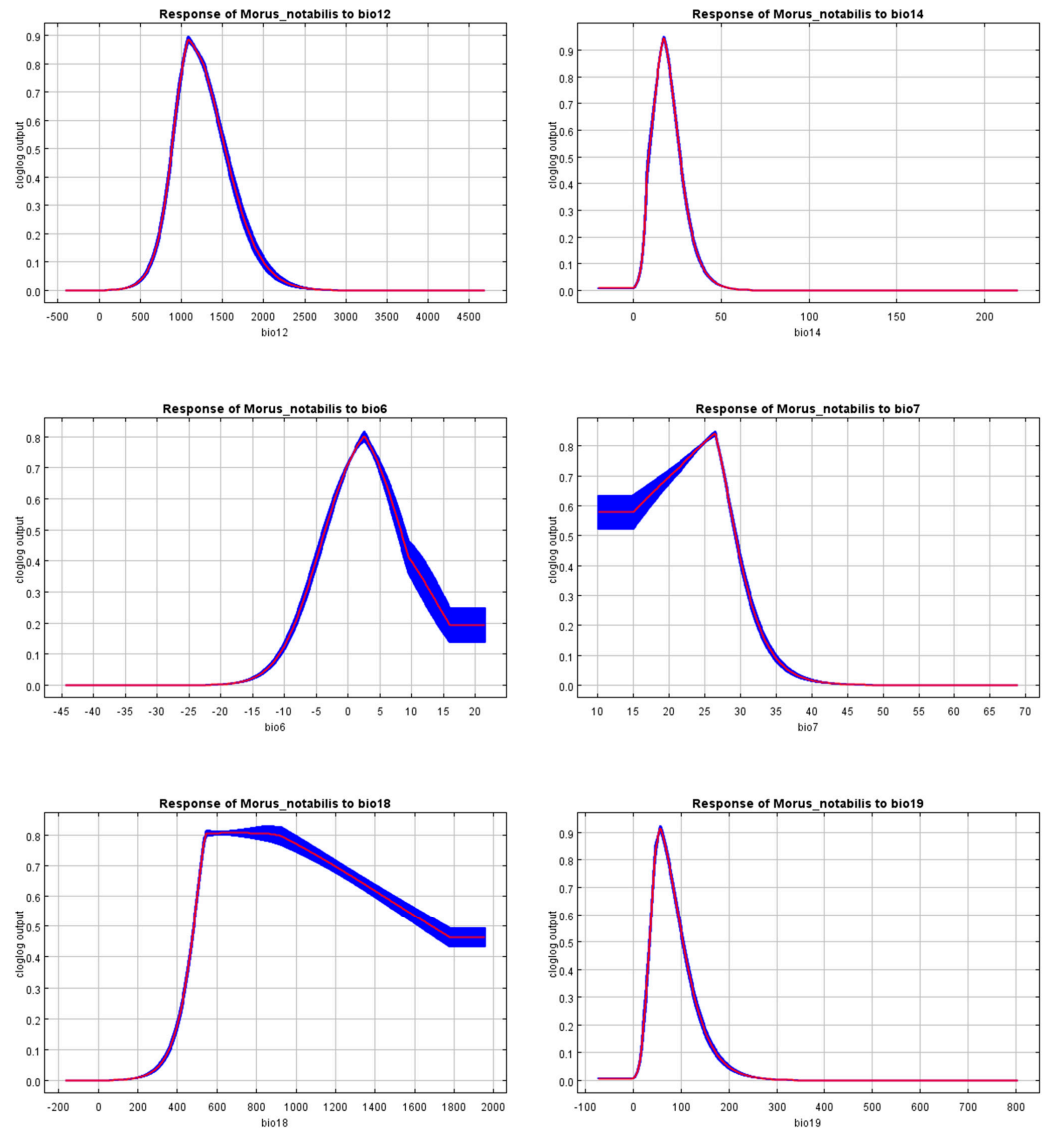


**Figure 7.** Response curves of the environmental variables that contributed most to the MaxEnt models. Red, the mean response of the 10 replicate Maxent runs. Blue, the mean  $\pm$  one standard deviation.

**Table 6.** A suitable range of environmental variables for the potential distribution of *Morus notabilis*.

Environmental Variables	Unit	Suitable Range	Optimum Value
Annual Precipitation (bio12)	mm	824.15–1682.20	1088.98
Precipitation of Driest Month (bio14)	Mm	6.94–30.27	17.37
Min Temperature of Coldest Month (bio6)	$^{\circ}\text{C}$	$-6.05$ – $12.05$	2.58
Temperature Annual Range (bio5–bio6) (bio7)	$^{\circ}\text{C}$	$10.00$ – $31.02$	26.50
Precipitation of Warmest Quarter (bio18)	Mm	448.09–1955	761.12
Precipitation of Coldest Quarter (bio19)	mm	27.53–124.09	56.68

#### 4. Discussion

The MaxEnt model was established in this study using 101 distribution sites for selected species and relevant environmental variables. The jackknife test analysis yielded an AUC value of 0.938, indicating high accuracy of the model's simulation results. Using the MaxEnt model, we determined the current geographical range of suitability distribution for *M. notabilis* and predicted its future changes in suitability distribution and environmental adaptation under varying concentrations [28].

The prediction results of the MaxEnt model indicate that the current highly suitable area for *M. notabilis* is primarily concentrated in Sichuan, with additional scattered distribution observed in Yunnan, Guizhou, Chongqing, and Hubei. The distribution of moderately suitable areas is mainly found in Yunnan, with a significant regional presence also observed in Sichuan, Guizhou, Chongqing, and Tibet. Conversely, low-suitability areas exhibit a relatively extensive distribution pattern encompassing Guangxi, Henan, and Shaanxi, as well as scattered regions across central China, South China, and Northwest China. While the low-suitability areas are dispersed throughout various locations, the moderately and highly suitable areas display notable concentration primarily within the renowned southwestern provinces and city of Sichuan, Yunnan, Guizhou, and Chongqing, respectively. These four provinces have cold air blocked by the Qinling Mountains and influenced by both East Asian monsoon and South Asian tropical monsoon systems, resulting in diverse climate types characterized by abundant natural resources along with high terrain towards the northwest transitioning to lower elevations towards the southeast [29]. The Sichuan Basin exhibits a subtropical monsoon humid climate, characterized by mild winters and hot summers, as well as distinct seasonal variations. The Yunnan-Guizhou Plateau is a subtropical humid region with minimal temperature fluctuations throughout the year but clearly defined dry and wet seasons. The climatic conditions in these four provinces and cities are highly favorable for plant growth, making them an optimal choice. *M. notabilis* has a limited distribution range and is typically found in mountain forests, canyons, mountain gullies, and mixed broad-leaved forests. It is evident that the selection of suitable climatic conditions for the growth environment of this species is quite stringent [30].

In the predicted 2050s and 2090s, the areas of high and low suitability are expected to expand under three different climate conditions, while the area of medium suitability is anticipated to decrease. Moreover, the highest increase in suitability is predicted under the climate conditions of a high SSP5-8.5 emissions scenario. Under the low concentration scenario, there was a minor change in *M. notabilis* suitability by less than 10%, with small changes and no significant regional expansion observed. However, under the high concentration scenario, there was a substantial increase in suitability with an increased area proportion ranging from 20% to 30%. SSP5-8.5 represents the highest greenhouse gas emission scenario, and it has been found that *M. notabilis* exhibits optimal growth effects under higher concentrations of greenhouse gases due to its photosynthetic capacity as well as its adaptation to warmer winters and hotter summers caused by carbon dioxide emissions-induced climate warming [31]. The predicted areas of high suitability mainly expanded towards Guizhou and Yunnan provinces, indicating that these regions will continue to be key habitats for *Morus notabilis* in future development [32,33].

In the course of this experiment, the jackknife test and Pearson correlation coefficient were employed to identify 9 significant climate variables out of the initial selection of 19. The growth environment of trees is influenced by numerous factors, with essential nutrients for tree growth primarily absorbed through the root system from the soil [34]. Hence, in addition to climate factors, this study also considered soil and other environmental variables. The MaxEnt model identified 10 crucial variables that affect the distribution of *M. notabilis* among these environmental factors: Annual Precipitation, Altitude, Min Temperature of Coldest Month, Human footprint, Temperature Annual Range (bio5–bio6), Precipitation of Coldest Quarter, ultraviolet-B radiation, Precipitation of Driest Month, Precipitation Warmest Quarter, and Soil reference depth. Similar findings were found when predicting other plant species with MaxEnt. The mean UV-B of the highest month, seasonality of pre-

precipitation, and human footprint were found to influence the distribution in the prediction of suitable areas for *Isoetes* by Yang et al. [35]. Annual precipitation and soil depth were found to influence the distribution in the prediction of *Ephedra* by He et al. [16]. Combining these findings with the jackknife test revealed that the most influential environmental variables are: Annual Precipitation, Precipitation Driest Month, Min Temperature Coldest Month, Temperature Annual Range (bio5–bio6), Precipitation Warmest Quarter, and Precipitation Coldest Quarter. The optimal range for these six influential environmental variables on potential forest distribution indicated that precipitation during mid-age had an optimum value of 1088.98 mm, precipitation during the driest month had an optimum value of 17.37 mm, precipitation during the warmest quarter had an optimum value of 761.12 mm, and precipitation in the coldest areas had an optimum value of 56.68 mm. The response curves for annual precipitation, precipitation in the driest month, and precipitation in the coldest area exhibited distinct peak shapes characterized by steep inclines and declines along a narrow variation interval. This suggests that *M. notabilis* has a limited suitable range for precipitation and possesses poor tolerance to droughts and floods under dry and cold air conditions [33,36].

In the warmest quarter, as precipitation decreased, the suitability of *M. notabilis* trees increased significantly until reaching an optimal amount of precipitation. Beyond this point, suitability slowly declined within a range of water amounts but still maintained a value of 0.47 in the end, indicating medium suitability for distribution [37]. Thus, while *M. notabilis* has poor drought tolerance in warm climates with full sunshine, its flood tolerance is significantly enhanced by rapid water evaporation [36]. The minimum temperature during the coldest month ranges from  $-6.05\text{ }^{\circ}\text{C}$  to  $12.05\text{ }^{\circ}\text{C}$  (with an optimal value of  $2.58\text{ }^{\circ}\text{C}$ ), and annual temperatures range from  $10.00\text{ }^{\circ}\text{C}$  to  $31.02\text{ }^{\circ}\text{C}$  (with an optimal value of  $26.50\text{ }^{\circ}\text{C}$ ). These small temperature ranges suggest that *M. notabilis* has limited adaptability to varying temperatures and may not be suitable for regions like Inner Mongolia or Xinjiang due to their harsh climate conditions characterized by low precipitation or large temperature differences between day and night, respectively [38]. For successful planting guidelines for *M. notabilis* trees, it is recommended that the soil be irrigated and well-drained with high fertility levels [39].

As a maximum entropy-based niche model, the MaxEnt model possesses several advantages over other prediction models, including its ability to accurately predict with small sample sizes and exhibit robust performance [40]. However, the MaxEnt model relies on known distribution data for target species and selected environmental variables to study the probability distribution of *M. notabilis* in a specific area [41,42]. The limited availability of relevant data for *M. notabilis* may impact the accuracy of the model's predictions to some extent. *M. notabilis* is a mulberry tree that is influenced by various factors, such as soil composition, climate conditions, light exposure, wind intensity, and air quality [43]. Although this study considers multiple environmental factors like climate, soil properties, ultraviolet radiation levels, organic carbon content, and human activities, it should be noted that species growth is influenced by numerous interacting variables, which were not comprehensively addressed in this paper [30,32]. Mulberry leaves serve as the primary feed for silkworms, while mulberry fruit has both medicinal and dietary uses. As society develops and demands for silk production change, along with alterations in mulberry leaf utilization and fruit consumption patterns [44], unpredictable effects from human activities on *M. notabilis* distribution may arise [44]. Therefore, future studies should update their predictions accordingly based on evolving circumstances [28].

## 5. Conclusions

Based on the existing distribution information of *M. notabilis* and selected environmental factors, combined with ArcGIS technology and the MaxEnt model, this study obtained the current suitable habitat distribution of *M. notabilis* and also predicted the change in suitability distribution and environmental adaptation of *M. notabilis* under different concentration climate conditions in the future. The results showed that the current and future

middle-high suitable areas of Sichuan and *M. notabilis* were mainly concentrated in the southwest of Sichuan, Yunnan, Guizhou, and Chongqing. In the scenario of high temperature chamber gas concentration SSP5-8.5, the percentage increase in the high suitability region was 25.52% and 29.74% in the 2050s and 2090s, respectively, and the growth of suitable habitat was the most obvious. The key environmental variables affecting the distribution of *M. notabilis* were Annual Precipitation (bio12), Precipitation of Driest Month (bio14), Min Temperature of Coldest Month (bio6), Temperature Annual Range (bio5–bio6) (bio7), Precipitation of Warmest Quarter (bio18), and Precipitation of Coldest Quarter (bio19). In this study, the influence of the MaxEnt model on the distribution of suitable habitat for *M. notabilis* was discussed, which provided some information for the planting of *M. notabilis* in agriculture. Further research will be carried out with updated information in the future.

**Author Contributions:** Conceptualization, H.G. and Q.Q.; methodology, D.X. and X.D.; software, Y.P.; investigation, H.G. and Q.Q.; writing—original draft, H.G. and X.D.; writing—review and editing, D.X. All authors have read and agreed to the published version of the manuscript.

**Funding:** This research was supported by the Sichuan Province Science and Technology Support Program (2022NSFSC0986), the China West Normal University Support Program (20A007, 20E051, 21E040, and 22kA011), and the earmarked fund for CARS-18.

**Data Availability Statement:** The data supporting the results are available in a public repository at: GBIF.org (accessed on 1 January 2024). GBIF Occurrence Download <https://doi.org/10.15468/dl.nqcv9> (accessed on 1 January 2024) and Qianqian Qian (2023): Locations of *Morus notabilis*.docx. figshare. Dataset. <https://doi.org/10.6084/m9.figshare.24902286> (accessed on 1 January 2024).

**Conflicts of Interest:** The authors declare no conflicts of interest.

## References

- Hou, C.; Chao, N.; Dai, M.; Liu, L. Screening of 4CL Family Genes in Mulberry and Functional Study of *Mm4CL2*. *Acta Sericol. Sin.* **2022**, *48*, 18–24.
- Zhou, Y. Preliminary Study on the Function of Mulberry *FBA380* and *FBK70* in Fruit Coloration. Master's Thesis, Southwest University, Chongqing, China, 2022.
- Liu, D.; Meng, S.; Xiang, Z.; He, N.; Yang, G. Antimicrobial mechanism of reaction products of *Morus notabilis* C.K. Schneid (mulberry) polyphenol oxidases and chlorogenic acid. *Phytochemistry* **2019**, *163*, 1–10. [[CrossRef](#)]
- Kılınçer, İ.; Khanyile, L.; Gürcan, K.; Şimşek, Ö.; Uzun, A.; Nikbakht-Dehkordi, A. Decaploid sour black mulberry (*Morus nigra* L.) in Western Asia: Features, domestication history, and unique population genetics. *Genet. Resour. Crop Environ.* **2023**, 1–18. [[CrossRef](#)]
- Zheng, S.; Zhu, Y.; Liu, C.; Fan, W.; Xiang, Z.; Zhao, A. Genome-wide identification and characterization of genes involved in melatonin biosynthesis in *Morus notabilis* C.K. Schneid (wild mulberry). *Phytochemistry* **2021**, *189*, 112819. [[CrossRef](#)] [[PubMed](#)]
- Vanhaelewyn, L.; Prinsen, E.; Van Der Straeten, D.; Vandenbussche, F. Hormone-controlled UV-B responses in plants. *J. Exp. Bot.* **2016**, *67*, 4469–4482. [[CrossRef](#)] [[PubMed](#)]
- Sun, Z.; Kumar, R.M.S.; Li, J.; Yang, G.; Xie, Y. In Silico search and biological validation of *MicroR171* family related to abiotic stress response in mulberry (*Morus alba* L.). *Hortic. Plant J.* **2022**, *8*, 184–194. [[CrossRef](#)]
- Liu, D.; Zeng, Y.; Qiu, C.; Lin, Q. Molecular Cloning and Adversity Stress Expression Analysis of SPDS Genes in Mulberry (*Morus notabilis* C.K. Schneid). *Russ. J. Plant Physiol.* **2021**, *68*, 1186–1193. [[CrossRef](#)]
- Sharma, R.; Khan, S.; Kaul, V. Predicting the potential habitat suitability and distribution of “Weed-Onion” (*Asphodelus tenuifolius* Cavan.) in India under predicted climate change scenarios. *J. Agric. Food Res.* **2023**, *14*, 100697. [[CrossRef](#)]
- Sekhar, K.M.; Reddy, K.S.; Reddy, A.R. Amelioration of drought-induced negative responses by elevated CO<sub>2</sub> in field grown short rotation coppice mulberry (*Morus* spp.), a potential bio-energy tree crop. *Photosynth. Res.* **2017**, *132*, 151–164. [[CrossRef](#)]
- Imani Wa Rusaati, B.; Won Kang, J. MaxEnt modeling for predicting the potential distribution of *Lebrunia bushaie* Staner (Clusiaceae) under different climate change scenarios in Democratic Republic of Congo. *J. Asia-Pac. Biodivers.* **2023**; in press. [[CrossRef](#)]
- Zhuo, Z.; Xu, D.; Pu, B.; Wang, R.; Ye, M. Predicting distribution of *Zanthoxylum bungeanum* Maxim. in China. *BMC Ecol.* **2020**, *20*, 46. [[CrossRef](#)]
- Liu, Z.; Zhou, P.; Zhang, F.; Liu, X.; Chen, G. Spatiotemporal characteristics of dryness/wetness conditions across Qinghai Province, Northwest China. *Agric. For. Meteorol.* **2013**, *182–183*, 101–108. [[CrossRef](#)]
- Xin, X.; Jiang, X.; Thomas, A.; Niu, B.; Zhang, M.; Xu, X.; Zhang, R.; Li, H.; Gui, Z. Studies on 1-deoxynojirimycin biosynthesis in mulberry (*Morus alba* L.) seeds through comparative transcriptomics. *Nat. Prod. Res.* **2023**, 1–10. [[CrossRef](#)] [[PubMed](#)]

15. Wu, B.; Zhou, L.; Qi, S.; Jin, M.; Hu, J.; Lu, J. Effect of habitat factors on the understory plant diversity of *Platycladus orientalis* (Linnaeus) plantations in Beijing mountainous areas based on MaxEnt model. *Ecol. Indic.* **2021**, *129*, 107917. [[CrossRef](#)]
16. He, P.; Li, J.; Li, Y.; Xu, N.; Gao, Y.; Guo, L.; Huo, T.; Peng, C.; Meng, F. Habitat protection and planning for three *Ephedra* using the MaxEnt and Marxan models. *Ecol. Indic.* **2021**, *133*, 108399. [[CrossRef](#)]
17. Thakur, S.; Rai, I.D.; Singh, B.; Dutt, H.C.; Musarella, C.M. Predicting the suitable habitats of *Elwendia persica* (Boiss.) in the Indian Himalayan Region (IHR). *Plant Biosyst.—Int. J. Deal. All Asp. Plant Biol.* **2023**, *157*, 769–778. [[CrossRef](#)]
18. Ji, W.; Gao, Y.; Wei, J. Potential Global Distribution of *Daktulosphaira vitifoliae* (Fitch) under Climate Change Based on MaxEnt. *Insects* **2021**, *12*, 347. [[CrossRef](#)] [[PubMed](#)]
19. Xia, Z.; Dai, X.; Fan, W.; Liu, C.; Zhang, M.; Bian, P.; Zhou, Y.; Li, L.; Zhu, B.; Liu, S.; et al. Chromosome-level Genomes Reveal the Genetic Basis of Descending Dysploidy and Sex Determination in *Morus* Plants. *Genom. Proteom. Bioinf.* **2022**, *20*, 1119–1137. [[CrossRef](#)] [[PubMed](#)]
20. Gao, H. Method of improving the conversion of Cadmium-containing plant biomass energy under the background of soil pollution. *Energy Rep.* **2022**, *8*, 10803–10811. [[CrossRef](#)]
21. Zhao, H.; Xian, X.; Guo, J.; Yang, N.; Zhang, Y.; Chen, B.; Huang, H.; Liu, W. Monitoring the little fire ant, *Wasmannia auropunctata* (Roger 1863), in the early stage of its invasion in China: Predicting its geographical distribution pattern under climate change. *J. Integr. Agric.* **2023**, *22*, 2783–2795. [[CrossRef](#)]
22. Li, X.; Xu, D.; Jin, Y.; Zhuo, Z.; Yang, H.; Hu, J.; Wang, R. Predicting the current and future distributions of *Brontispa longissimi* (Gestro) (Coleoptera: Chrysomelidae) under climate change in China. *Glob. Ecol. Conserv.* **2020**, *25*, e1444. [[CrossRef](#)]
23. Xu, D.; Zhuo, Z.; Li, X.; Wang, R. Distribution and invasion risk assessment of *Oryctes rhinoceros* (L.) in China under changing climate. *J. Appl. Entomol.* **2022**, *146*, 385–395. [[CrossRef](#)]
24. Islam, K.N.; Rana, L.R.S.; Islam, K.; Hossain, M.S.; Hossain, M.M.; Hossain, M.A. Climate change and the distribution of two *Ficus* spp. in Bangladesh—Predicting the spatial shifts. *Trees For. People* **2021**, *4*, 100086. [[CrossRef](#)]
25. Wan, J.; Qi, G.; Ma, J.; Ren, Y.; Wang, R.; McKirdy, S. Predicting the potential geographic distribution of *Bactrocera bryoniae* (Tryon) and *Bactrocera neohumeralis* (Hardy) (Diptera: Tephritidae) in China using MaxEnt ecological niche modeling. *J. Integr. Agric.* **2020**, *19*, 2072–2082. [[CrossRef](#)]
26. Yuyuan, X.; Chen, L.; Ningning, Z.; Wencheng, L.; Jingyuan, S.; Xuehong, W. Prediction of Suitable Habitat of Tibetan Migratory Locust in Changdu City Based on MaxEnt Model. *J. Plateau Agric.* **2023**, *7*, 249–258. [[CrossRef](#)]
27. Maurya, A.; Semwal, M.; Mishra, B.P.; Mohan, R.; Rana, T.S.; Nair, N.K. Distribution modeling for predicting habitat suitability for citron (*Citrus medica* L.) under climate change scenarios. *Flora* **2023**, *304*, 152298. [[CrossRef](#)]
28. Shishir, S.; Mollah, T.H.; Tsuyuzaki, S.; Wada, N. Predicting the probable impact of climate change on the distribution of threatened *Shorea robusta* Gaertn. f. forest in Purbachal, Bangladesh. *Glob. Ecol. Conserv.* **2020**, *24*, e1250. [[CrossRef](#)]
29. Xu, D.; Zhuo, Z.; Wang, R.; Ye, M.; Pu, B. Modeling the distribution of *Zanthoxylum armatum* DC. in China with MaxEnt modeling. *Glob. Ecol. Conserv.* **2019**, *19*, e691. [[CrossRef](#)]
30. Cheng, Z.; Aakala, T.; Larjavaara, M. Elevation, aspect, and slope influence woody vegetation structure and composition but not species richness in a human-influenced landscape in northwestern Yunnan, China. *Front. Glob. Chang.* **2023**, *6*, 1187724. [[CrossRef](#)]
31. Jain, M.; Bansal, J.; Rajkumar, M.S.; Sharma, N.; Khurana, J.P.; Khurana, P. Draft genome sequence of Indian mulberry (*Morus indica* L.) provides a resource for functional and translational genomics. *Genomics* **2022**, *114*, 110346. [[CrossRef](#)]
32. Brunel, N.; Meza, F.; Ros, R.; Santibáñez, F. Effects of topsoil loss on wheat productivity in dryland zones of Chile. *J. Soil Sci. Plant Nutr.* **2011**, *11*, 129–137. [[CrossRef](#)]
33. Ries, G.; Heller, W.; Puchta, H.; Sandermann, H.; Seidlitz, H.K.; Hohn, B. Elevated UV-B radiation reduces genome stability in plants. *Nature* **2000**, *406*, 98–101. [[CrossRef](#)]
34. Angst, G.; Messinger, J.; Greiner, M.; Häusler, W.; Hertel, D.; Kirfel, K.; Kögel-Knabner, I.; Leuschner, C.; Rethemeyer, J.; Mueller, C.W. Soil organic carbon stocks in topsoil and subsoil controlled by parent material, carbon input in the rhizosphere, and microbial-derived compounds. *Soil Biol. Biochem.* **2018**, *122*, 19–30. [[CrossRef](#)]
35. Yang, J.; Huang, Y.; Jiang, X.; Chen, H.; Liu, M.; Wang, R. Potential geographical distribution of the edangered plant *Isoetes* under human activities using MaxEnt and GARP. *Glob. Ecol. Conserv.* **2022**, *38*, e2186. [[CrossRef](#)]
36. Naasko, K.I.; Naylor, D.; Graham, E.B.; Couvillion, S.P.; Danczak, R.; Tolic, N.; Nicora, C.; Fransen, S.; Tao, H.; Hofmockel, K.S.; et al. Influence of soil depth, irrigation, and plant genotype on the soil microbiome, metapenome, and carbon chemistry. *mBio* **2023**, *14*, e175823. [[CrossRef](#)]
37. Soilhi, Z.; Sayari, N.; Benalouache, N.; Mekki, M. Predicting current and future distributions of *Mentha pulegium* L. in Tunisia under climate change conditions, using the MaxEnt model. *Ecol. Inform.* **2022**, *68*, 101533. [[CrossRef](#)]
38. Gruber, H.; Ulm, R.; Heijde, M. Regulation of UV-B-induced photomorphogenesis in Arabidopsis. *Comp. Biochem. Physiol. A-Mol. Integr. Physiol.—Comp. Biochem. Physiol. Part A* **2009**, *153*, S200. [[CrossRef](#)]
39. Wiśniewski, P.; Märker, M. Comparison of Topsoil Organic Carbon Stocks on Slopes under Soil-Protecting Forests in Relation to the Adjacent Agricultural Slopes. *Forests* **2021**, *12*, 390. [[CrossRef](#)]
40. Hyyryläinen, A.; Turunen, M.; Rautio, P.; Huttunen, S. Sphagnum mosses in a changing UV-B environment: A review. *Perspect. Plant Ecol. Evol. Syst.* **2018**, *33*, 1–8. [[CrossRef](#)]

41. Swart, C.; Donaldson, J.; Barker, N. Predicting the distribution of *Encephalartos latifrons* (Lehmann), a critically endangered cycad in South Africa. *Biodivers. Conserv.* **2018**, *27*, 1961–1980. [[CrossRef](#)]
42. Mapunda, K.K.; Andrew, S.M. Predicting the distribution of critically endangered tree species *Karomia gigas* (Faden) under climate change in Tanzania. *Ecol. Eng.* **2023**, *195*, 107065. [[CrossRef](#)]
43. Yost, M.A.; Kitchen, N.R.; Sudduth, K.A.; Thompson, A.L.; Allphin, E. Topsoil Thickness Influences Nitrogen Management of Switchgrass. *Bioenerg. Res.* **2017**, *10*, 465–477. [[CrossRef](#)]
44. Cajigas Gandia, A.; Alonso Bosch, R.; Mancina, C.A.; Herrel, A. Climatic variation along the distributional range in Cuban *Anolis* lizards: Species and ecomorphs under future scenarios of climate change. *Glob. Ecol. Conserv.* **2023**, *42*, e2401. [[CrossRef](#)]

**Disclaimer/Publisher’s Note:** The statements, opinions and data contained in all publications are solely those of the individual author(s) and contributor(s) and not of MDPI and/or the editor(s). MDPI and/or the editor(s) disclaim responsibility for any injury to people or property resulting from any ideas, methods, instructions or products referred to in the content.